https://doi.org/10.2352/ISSN.2169-2629.2017.32.65

Evaluating Robustness of the Method to Estimate Five Components from Skin Spectral Image

Rina Akaho, Misa Hirose, Munenori Fukunishi and Norimichi Tsumura
Graduate School of Advanced Integration Science, Chiba University, CHIBA, JAPAN

Abstract

In this research, we evaluate robustness for noise and change of epidermis thickness in the method to estimate five components that are melanin, oxy-hemoglobin, deoxy-hemoglobin, shading and surface reflectance from spectral reflectance of skin at 5 wavelengths. We also estimated the five components from measured image of age spot and circles under eyes using the method. As a result of evaluation, we found that the noise of image is required to be 0.1% or less to accurately estimate five components and the thickness of epidermis affects the estimated value. However, we could acquire the distribution of major causative for age spot and circle under eyes by applying the method to measured spectral images.

Introduction

Skin is three-layered tissue composed of epidermis, dermis and subcutaneous tissues and has chromophores such as melanin, oxyhemoglobin and deoxyhemoglobin. Diffuse reflectance of human skin is changed five components shading and surface reflectance due to the shape of face adding these three chromophores. The analysis of diffuse reflectance provide us the information on tissue activities related to chromophores. These information can be applied to early detection of skin disease and monitoring health.Methods of estimating four components except the surface reflection were proposed as follows. N. Tsumura *et al.* discussed the method of extracting melanin and hemoglobin by applying independent component analysis to skin color image [1]. J. Kikuchi *et al*. proposed imaging of hemoglobin oxygen saturation ratio in the face by spectral camera based on multi regression analysis [2]. A lot of studies have been performed as above methods for estimating four components except the surface reflection linearly from skin color image and spectral image. On the other hand, M. Kobayashi *et al*. analyzed nonlinear relation between absorbance and chromophores of skin based on Monte Carlo simulation and modified Lambert beer's law and reported method of estimating optical path length each layer from absorbance and the amount of chromophores and shading [3]. By using the estimated optical path length, the concentration of chromophores can be analyzed based on Modified Lambert Beer's law. However, this method cannot estimate the optical path length if the concentration of chromophores are not given. Even if the concentration is known, the estimation accuracy is not sufficient since the concentration is derived linearly by multiple regression analysis. Therefore, Hirose et al. proposed a new nonlinear estimation method for unknown three chromophore concentrations, shading and surface reflection from spectral reflectance at five wavelengths of skin [4]. However, toward practical use, it is necessary to evaluate robustness of the method and apply the method to measured five band image of skin.

In this paper, therefore, we evaluate robustness for noise and change of epidermis thickness in the method to estimate five components. Monte Carlo simulation is used to evaluate the robustness. We also estimated five components from measured five band image. Images of age spot and circle under eyes are captured and analyzed.

Method of Estimating Five Components [4]

Analysis of the Relation between Absorbance and Chromophore Concentration

Hirose et al. analyze the relation between absorbance and chromophore concentrations by using Monte Carlo simulation [3]. First, we obtain diffuse reflectance data for skin by Monte Carlo simulation of light transport in multi-layered tissue (MCML) proposed by Jacques S. L. *et al.* [5]. MCML is constituted by following the propagation of photons in tissue. As shown in Fig.1, we assumed two-layered skin model composed of epidermis and dermis. The five optics parameters are set at each layer such as thickness t, reflectance index n, anisotropy factor g, scattering coefficient μ_s and absorption coefficient μ_a. The thickness t of epidermis and dermis are 0.006 and 0.40 cm respectively in this research. The reflectance index n, scattering coefficient μ_s and anisotropy factor g of two layers are the same value, n = 1.4, μ_s and g are shown in Fig.2 [6]. The absorption coefficient μ_a is calculated by the absorption coefficients of chromophores such as melanin, oxy-hemoglobin and deoxy-hemoglobin as follows.

$$\begin{aligned}\mu_{a.epi}(\lambda) &= [Mel]\mu_{a.mel}(\lambda),\\ \mu_{a.der}(\lambda) &= [Ohb]\mu_{a.ohb}(\lambda)+[Hb]\mu_{a.hb}(\lambda)\\ &= [Thb][StO]\mu_{a.ohb}(\lambda)+[Thb](1-[StO])\mu_{a.hb}(\lambda),\end{aligned} \quad (1)$$

where λ is wavelength and the subscript of absorption coefficient *epi*, *der*, *mel*, *ohb* and *hb* indicate epidermis, dermis, melanin, oxy-hemoglobin and deoxy-hemoglobin respectively. The absorption coefficients of chromophores are shown in Fig.3 [6]. The percentage of melanin, oxy-hemoglobin and deoxy-hemoglobin are expressed by [*Mel*], [*Ohb*] and [*Hb*] respectively. We input these percentage of chromophores to MCML and acquire diffuse reflectance of skin $R_{MCML}(\lambda)$. The percentage of oxy-hemoglobin and deoxy-hemoglobin are calculated by blood volume [*Thb*] and oxygen saturation [*StO*]. The blood volume is defined by the sum

of oxy-hemoglobin and deoxy-hemoglobin, [*Ohb*] + [*Hb*]. The oxygen saturation indicates the ratio of oxy-hemoglobin in the blood and expressed by [*Ohb*]/([*Ohb*]+[*Hb*]). We set [*Mel*] = 1, 2, 3, 4, 5, 6, 7, 8, 9, 10%, [*Thb*] = 0.2, 0.4, 0.6, 0.8, 1.0%, [*StO*] = 0, 20, 40, 60, 80, 100%, and acquire 300 reflectance data from their combinations.

Next, Hirose et al. convert the reflectance $R_{MCML}(\lambda)$ to absorbance $Abs_{MCML}(\lambda)$ by $-log(R_{MCML}(\lambda))$. The relation between the absorbance for 560, 570, 590, 610 and 700 nm and chromophore concentrations are shown in Fig.4. The *Z*-axis represents the absorbance, the *X*-axis and *Y*-axis are defined by the absorption coefficient of dermis $\mu_{a.der}(\lambda)$ and the percentage of melanin [*Mel*]. The red dots in Fig.4 indicate the 300 absorbance data $Abs_{MCML}(\lambda)$ obtained by MCML. To obtain the well fitted curves for 300 absorbance data, we model the absorbance *Z* by a cubic function of *X* and *Y* for each wavelength as follows.

$$Z = AX^3 + BX^2Y + CXY^2 + DY^3 + EX^2 + FXY + GY^2 + HX + IY + J, \quad (2)$$

where *X* is $\mu_{a.der}(\lambda)$ as defined in Eq.(1) and *Y* is percentage of melanin [*Mel*]. The coefficient *A* to *J* are determined to minimize the residual sum of squares RSS_{func} for each wavelength.

$$RSS_{func}(\lambda) = \sum_{i=1}^{300} [Abs_{MCML}(\lambda, i) - Z(\lambda)]^2, \quad (3)$$

where $Abs_{MCML}(i)$ indicates *i-th* absorbance generated by MCML.

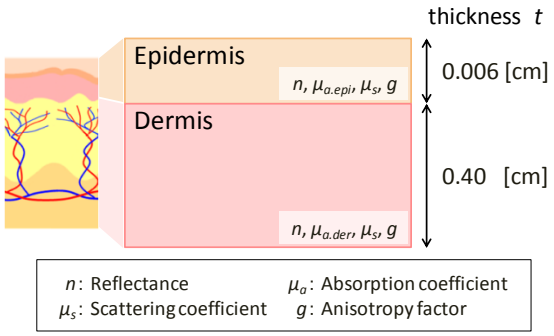

Figure 1. *Two-layered skin model composed of epidermis and dermis*

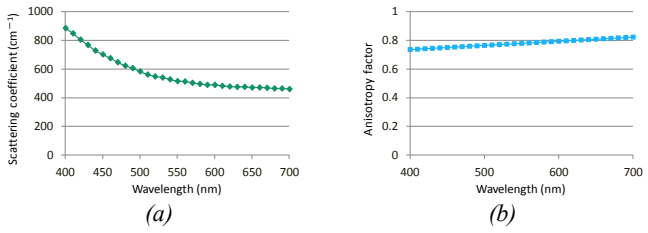

Figure 2. *(a) is scattering coefficient and (b) is anisotropy factor.*

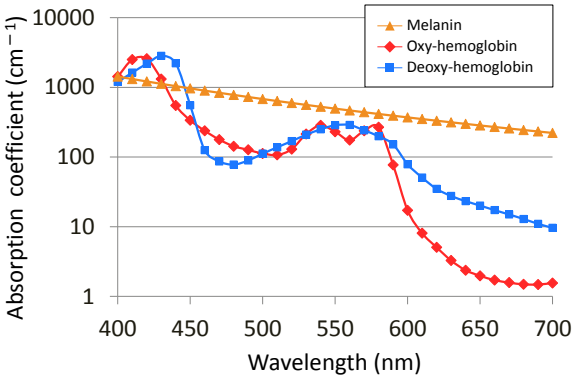

Figure 3. *Absorption coefficient of chromophores that are melanin, oxy-hemoglobin and deoxy-hemoglobin [7]*

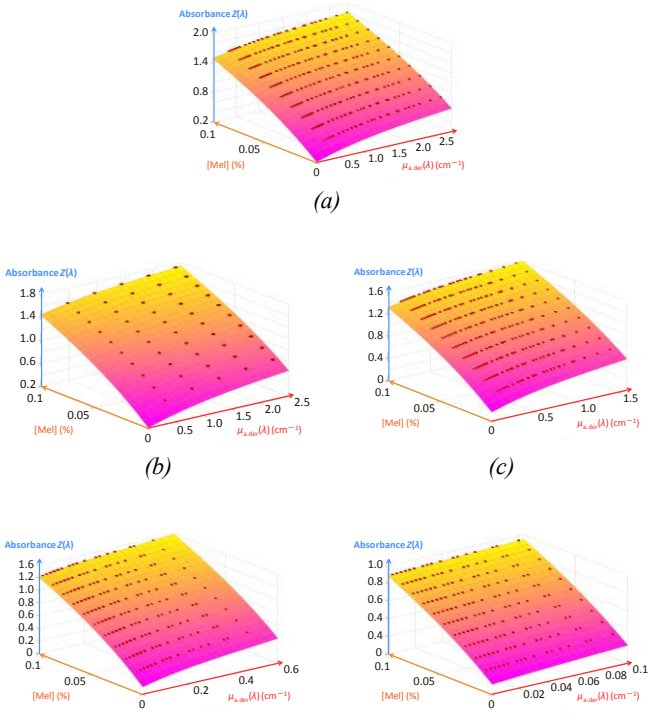

Figure 4. *Nonlinear relation between Monte Carlo simulation and chromophore concentration at five wavelengths: (a)560nm, (b)570nm, (c)590nm, (d)610nm, (e)700nm*

Estimation of Chromophore Concentrations, Shading and Surface Reflectance from Five Band Images

Hirose et al. then propose to extract five components that are melanin, oxy-hemoglobin, deoxy-hemoglobin, shading and surface reflection from five band images of skin by using the cubic function $Z(\lambda)$ represented by Eq. (2). It is assumed that five components estimated from spectral reflectance of skin $R(\lambda)$. Incident light is deflected or absorbed. The light incident on the skin is divided into surface reflection reflected by the skin surface and diffuse reflection scattered and absorbed by the chromophores in Fig.5. It is noted that the relationship between the diffuse reflection $R_{df}(\lambda)$ and absorption $A(\lambda)$ is shown as follows.

$$A(\lambda) = -\log(R_{df}(\lambda)). \tag{4}$$

In Lambert-Beer law, absorbance $A(\lambda)$ can be calculated from the cubic function of absorbance $Z(\lambda)$ and shading k as follows. The cubic function of absorbance $Z(\lambda)$ is defined in the concentration of three chromophores in Eq.(2).

$$A(\lambda) = Z(\lambda) + k. \tag{5}$$

Diffuse reflection $R_{df}(\lambda)$ is calculated from Eq.(4) and Eq.(5) as follows.

$$R_{df}(\lambda) = \exp(-(Z(\lambda) + k)). \tag{6}$$

Therefore, spectral reflectance of skin $R'(\lambda)$ is defined using surface reflectance R_{sp}.

$$\begin{aligned} R'(\lambda) &= R_{df}(\lambda) + R_{sp} \\ &= \exp(-(Z(\lambda) + k)) + R_{sp}. \end{aligned} \tag{7}$$

In the method, five components are determined to minimize the residual sum of squares RSS_{est} as follows.

$$RSS_{est} = \sum_{\lambda} [R(\lambda) - (\exp(-(Z(\lambda) + k)) + R_{sp})]^2, \tag{8}$$

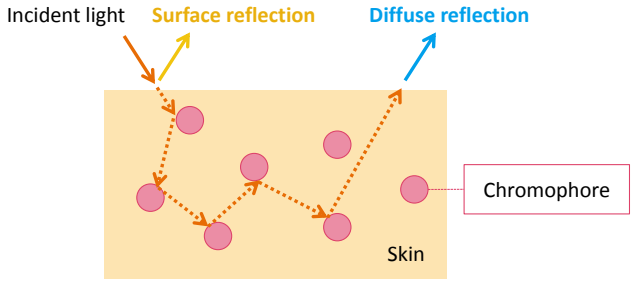

Figure 5. *Reflection properties of the skin*

Evaluation of noise robustness of the method

Spectral reflectance are simulated by Monte Carlo simulation. We set melanin concentration [*Mel*] = 1, 2, 3, 4, 5, 6, 7, 8, 9, 10%, blood volume [*Thb*] = 0.2, 0.4, 0.6, 0.8, 1.0%, oxygen saturation [*StO*] = 0, 20, 40, 60, 80, 100%, and acquire 300 reflectance data from their combinations. We add shading, surface reflection to the simulated reflectance. The noise is added randomly.

The average relative error and the correlation coefficient between the correct value and the estimated value are shown in Fig.6. Spectral reflectance data without noise is defined in "No-noise", with noise less than 0.1% is "less than 0.1%", with noise less than 1.0% is "less than 1.0%". In the case of "less than 0.1%", the average relative error of all components is less than 100%, and the correlation coefficient is more than 70%. However, when the noise exceeds 0.1%, the average relative error of shading and surface reflection become large and correlation is low in all components. Therefore, the noise of image is required to be 0.1% or less to accurately estimate five components.

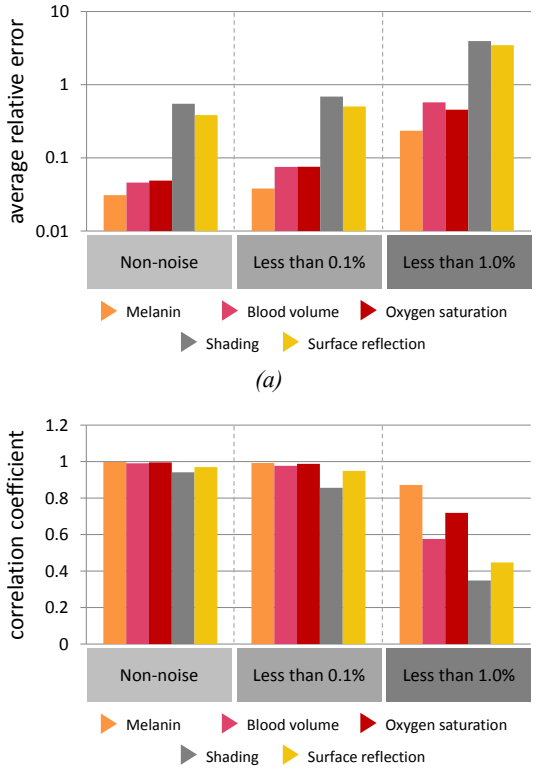

Figure 6. *Average relative error and correlation coefficient between the correct value and the estimated value: (a) average relative error, (b) correlation coefficient*

Evaluation of estimated result of the method when the thickness of epidermis is changed

The cubic function $Z(\lambda)$ is calculated based on Monte Carlo simulation to estimate five components. It is noted that the thickness of epidermis is set as 0.006[cm](60[μm]). Therefore, the cubic function $Z(\lambda)$ is absorbance of skin that has the thickness of epidermis 60[μm]. However, the thickness of epidermis is different depending on the parts as shown in Table.1 [8]. It is necessary to evaluate the estimated result when the thickness of epidermis is different from skin model. We generate numerical phantoms with various thickness of epidermis and evaluate estimated results.

Table.1 Mean thickness of epidermis [8]

Body Site	Mean Thickness [mm]
Palm	429.0
Fingertip	369.0
Back of hand	84.5
Forearm	60.9
Upper arm	43.9
Thoracic region	37.6
Abdomen	46.6
Upper back	43.4
Lower back	43.2
Thigh	54.3
Calf	74.9
Forehead	50.3
Cheek	38.8

Generating Numerical Phantom for Spectral Reflectance Map [4]

To demonstrate the effectiveness of the method, numerical phantom is required since the chromophore concentration is unknown in the actual skin spectral reflectance. In this research, we build, numerical phantom by generating spectral reflectance map with MCML. The outline of generating spectral reflectance map is shown in Fig.7.

First, in order to obtain the distribution of chromophores close to real skin, we extract chromophore component by applying independent component analysis on actual skin color image without surface reflection [1]. We capture this image by setting polarization filters in front of the camera and positioning the light sources to be parallel to each other. The obtained melanin concentration is divided into 3 and allocated input melanin concentration of MCML [*Mel*] = 3, 6, 9%. Similarly, the obtained hemoglobin concentration is divided into 3 and allocated input blood volume of MCML [*Thb*] = 0.2, 0.6, 1.0%. We also consider two oxygen saturation [*StO*] = 70, 100% and set lower oxygen saturation in the center of map. It is noted that this region intend to represent dark shadows under the eyes. To generate diffuse reflectance map, we assign diffuse reflectance from MCML corresponding to the combination of melanin concentration, blood volume and oxygen saturation to each pixel.

Next, we multiply shading to the diffuse reflectance map for generating the images that is constructed from four components. By adding surface reflectance on this four components image, we can generate the images that are constructed from five components. The surface reflectance is calculated by the subtraction between skin color image with and without surface reflection.

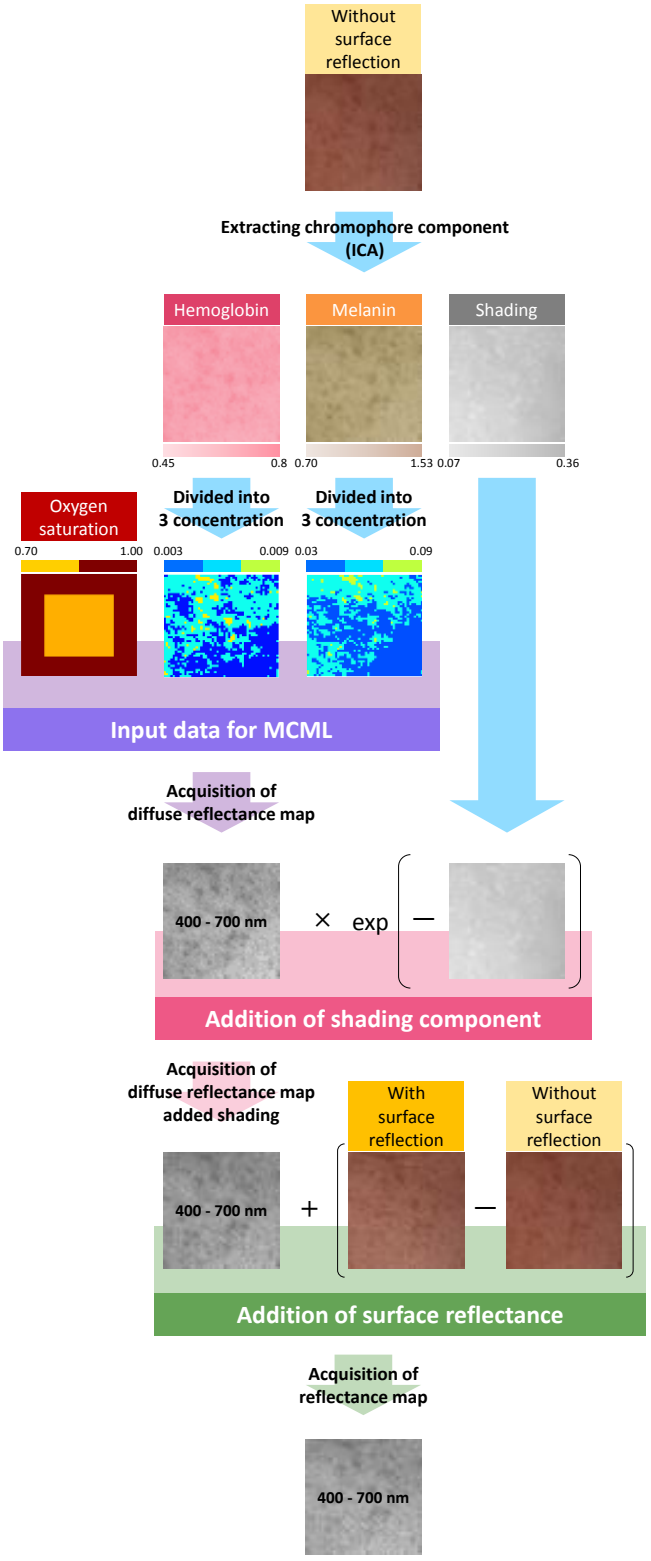

Figure 7. *Outline of generating spectral reflectance map*

Evaluating estimated result of our method when the thickness of epidermis is changed

We evaluate estimated results of our method when the thickness of epidermis is changed. As shown in Table.1, the thickness of epidermis of the palm and fingertip is thicker compared with the other sites, but that of most sites are from 20 to 100[μm]. Therefore, the numerical phantom was generated when the thickness of epidermis is 20, 30, 40, 50, 60, 70, 80, 90, 100[μm]. The five components estimated from numerical phantom is shown in Fig.8. In the case of 60[μm] (that is the same thickness as when we calculated the cubic function of absorbance $Z(\lambda)$ for estimation), estimated distribution and value of all components is also close to the correct value. When the thickness of epidermis is very thin, estimated value has an outlier. If the thickness of the skin is different from 60μm, the absolute error of the estimated value is increased but the tendency of distribution is almost unchanged. Therefore, although it is necessary to generate a cubic function $Z(\lambda)$ for each thickness in order to obtain the absolute value of concentration, there is no need that to obtain a rough distribution.

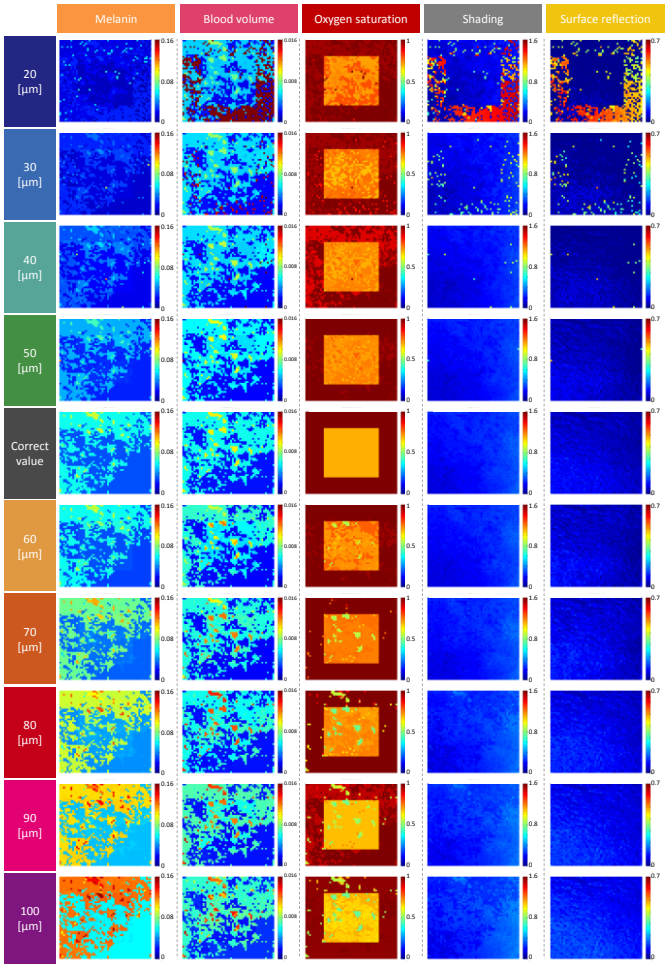

Figure 8. *Concentration distribution of five components when the thickness of epidermis is changed*

Estimation from measured five band image

Acquisition of facial image

Facial image was acquired to estimate five components from five band image by using the method. Experimental environment is shown in Fig.9. Lighting is a sun illuminating lamp SOLAX XC-500 (SERIC, Tokyo, Japan). Spectral camera is ImSpector (JFE Techno Research, Tokyo, Japan). Facial image was acquired in a visible region of 400-700nm. We use information in five wavelength 560nm, 570nm, 590nm, 610nm, 700nm to estimate components. Figure.10 and 11 shows measured image. To evaluate the estimated results, we captured image of age spot and circle under eyes.

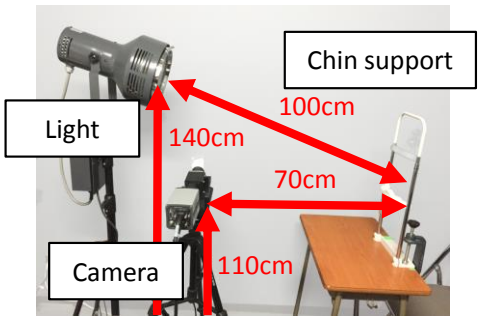

Figure 9. *Experiment environment for acquiring facial image*

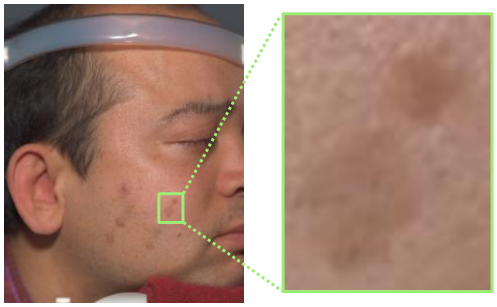

Figure 10. *Image of age spot*

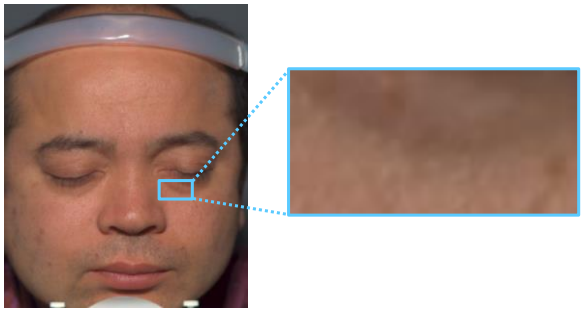

Figure 11. *Image of circle under eyes*

Estimated results from measured five band image

Figure 12 shows the estimated results from measured five band image of age spot using their method. The cause of the age spot is an increase of melanin. The distribution of melanin concentration is high in a region of age spot. Except for the region where the value is saturated, blood volume and oxygen saturation is substantially constant throughout.

Figure 13 shows the estimated results of circle under eyes. From Fig.13, the concentration of melanin is high at the top and bottom of circle under eyes and shading is seen throughout. In addition, the blood volume increases toward the inner corner of the eye. This tendency has been demonstrated experimentally [9]. Since the oxygen saturation indicates lower value throughout, the concentration of deoxyhemoglobin is high in the inner corner of eye. Therefore, we found that the cause of circle under eyes is the increase of melanin, oxy-hemoglobin and shading. In comparison with measured image and estimated distribution of surface reflection, we can see that gloss is acquired.

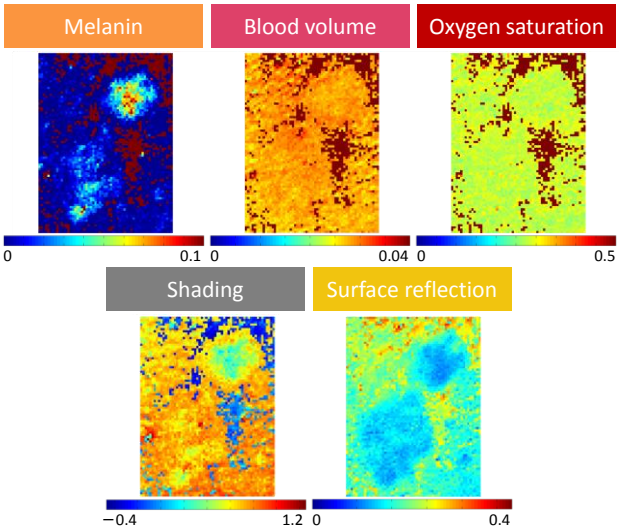

Figure 12. *Estimated concentration distribution of five components from image of age spot*

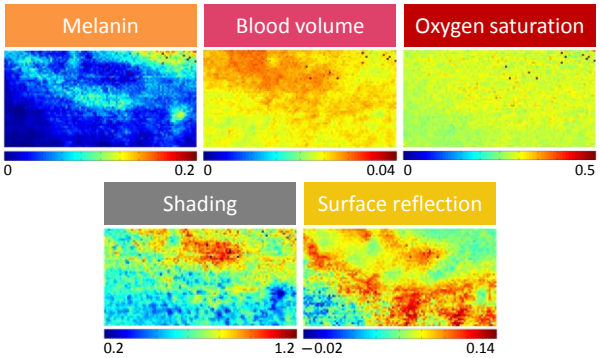

Figure 13. *Estimated concentration distribution of five components from image of circle under eyes*

Conclusion

In this paper, we evaluated robustness for noise and change of epidermis thickness in the method to estimate five components that are melanin, oxy-hemoglobin, deoxy-hemoglobin, shading and surface reflectance from spectral reflectance of skin at 5 wavelengths. As a result, we found that the noise of image is required to be 0.1% or less to accurately estimate five components. The thickness of epidermis affects the estimated value, but rough distribution of five components can be obtained. We also estimated five components from captured image of age spot and circles under eyes using our method. The distribution of major causative for age spot and circle under eyes can be acquired by applying our method to measured images. As a future work, it is necessary to speed up a program toward practical use.

References

[1] N. Tsumura, N. Ojima, K. Sato, et al., “Image-based skin color and texture analysis/synthesis by extracting hemoglobin and melanin information if the skin”, ACM Transactions on Graphics, Vol.22, No.3, 770-779 (2003).

[2] K. Kikuchi, Y. Masuda, T.Hirao, “Imaging of hemoglobin oxygen saturation ratio in the face by spectral camera and its application to evaluate dark circles”, Skin Research and Technology, Vol.19, 499-507 (2013).

[3] M. Kobayashi, Y. Ito, N. Sakauchi, et al., “Analysis of nonlinear relation for skin hemoglobin imaging”, Optical Society of America, Vol.9, No.13, 802-812 (2001).

[4] Misa Hirose and Norimichi Tsumura, "Nonlinear Estimation of Chromophore Concentrations, Shading and Surface Reflectance from Five Band Images", Color and Imaging Conference, Darmstadt, Germany, Proceedings pp.161-166, (10,2015)

[5] Wang L. and Jacques S. L., “Monte Carlo Modeling of Light Transport in Multi-layered Tissues in Standard C”, University of Texas M. D. Anderson Cancer Center (1992).

[6] N. Tsumura, M. Kawabuchi, H. Haneishi and Y. Miyake, “Mapping pigmentation in human skin from multi-channel visible spectrum image by inverse optical scattering technique”, Journal of Imaging Science and Technology, Vol.45, No.5, pg.444-450 (2000).

[7] Oregon Medical Laser Center, Optical Propetries Spectra, http://omlc.org/spectra/

[8] G. Poirier, “Human skin modelling and rendering”, M.S. Thesis, University of Waterloo, (2003).

[9] M. Matsumoto, N. Kobayashi and O. Hoshina, et al., “Study of Causal Factors of Dark Circles Around the Eyes”, IFSCC Magazine, 281-286, (2001).

Author Biography

Rina Akaho was born in Fukuoka, Japan, on 11 September 1993. She received the B.E degrees in Chiba University in 2016. She is interested in the color image processing, computer vision, computer graphics and biomedical optic